Neuroscience 170 (2010) 1223–1238

TRI-DIMENSIONAL AND TRIPHASIC MUSCLE ORGANIZATION OF WHOLE-BODY POINTING MOVEMENTS

E. CHIOVETTO,[a,b] B. BERRET[a] AND T. POZZO[a,c,d]*

[a]*Italian Institute of Technology, Via Morego 30, 16163 Genoa, Italy*

[b]*Department of Communication, Computer and System Sciences–University of Genoa, Via dell' Opera Pia 13, 16145 Genoa, Italy*

[c]*Université de Bourgogne, Dijon, Campus Universitaire, UFR Sciences et Techniques des Activitiés Physiques et Sportives, BP 27877, F-21078 Dijon, France*

[d]*INSERM, U887, Motricité-Plasticité, Dijon, F-21078, France*

Abstract—Previous kinematic and kinetic studies revealed that, when accomplishing a whole-body pointing task beyond arm's length, a modular and flexible organization could represent a robust solution to control simultaneously target pointing and equilibrium maintenance. Here, we investigated the underlying mechanisms that produce such a coordinative kinematic structure. We monitored the activity of a large number of muscles spread throughout subjects' bodies while they performed pointing movements beyond arm's length, either with or without imposition of postural or pointing constraints. Analyses revealed that muscle signals lied on a tri-dimensional hyper-plane and were temporally organized according to a triphasic pattern (three components, each one exhibiting one single peak of activation and the peaks being consecutive in time). Such a functional muscle synergy was found to be robust across conditions. Also the activities of the separate groups of muscles acting at each body joint resulted tri-dimensional. In particular, those associated with the muscles of the lower-body joints (ankle, knee and hip) always presented the three sequences in all conditions. However, a slightly different organization was found for the muscle activities of the upper-limb, suggesting a moderate level of flexibility of the activity of such muscles to movement constraints. The present findings link together, in a hierarchical view of motor control, the joint coordination characterizing whole-body pointing movements with a basic muscle synergistic organization, namely a triphasic pattern.

*Correspondence to: T. Pozzo, Université de Bourgogne, Dijon, Campus Universitaire, UFR STAPS, BP 27877, F-21078 Dijon, France. Tel: +33-380396756; fax: +33-380396702.
E-mail address: thierry.pozzo@u-bourgogne.fr (T. Pozzo).

Abbreviations: AL, adductor longus; A-P, antero–posterior centre of mass displacement; BF, biceps femoris; Bic, biceps femoris; Bra, brachioradialis; DA, deltoid anterior; DP, deltoid posterior; D1, target distance 1; D2, target distance 2; EMG, electromyographic signals; ES, erector spinae; Gast, gastrocnemius; GM, gluteus maximus; IT, imposed trajectory; K, no knee flexion; LD, latissimus dorsi; MD, movement duration; NNMF, nonnegative matrix factorization; OI, internal oblique; PC, principal component; PCA, principal component analysis; Pect, pectoralis major; Per, peroneus; PV, peak of velocity; RA, rectus abdominis; RF, rectus femoris; Rho, rhomboidus; Ser, serratus; SM, semitendinosus; Sol, soleus; ST, semimembranosus; Tib, tibialis; TPV, time to peak velocity; Tri, triceps; VAF, variance accounted for; Vert, vertical centre of mass displacement; VL, vastus lateralis; VM, vastus medialis.

Key words: EMG, muscle synergies, triphasic pattern, principal component analysis, non-negative matrix factorization, complex movements.

There is a growing amount of experimental evidences supporting the idea that the motor system use a narrow set of solutions to achieve complex actions. Therefore, specific strategies (usually referred to as synergies) would simplify the motor command by grouping together kinematic or muscle variables so as to reduce the dimension of the control space. For instance, low-dimensional organizations has been found to assemble muscular activity in the case of arm (d'Avella et al., 2006), head (Kakei et al., 1994; Sugiuchi et al., 2004), equilibrium tasks (Welch and Ting 2008; Krishnamoorthy et al., 2003; Danna-Dos-Santos et al., 2008) and locomotion (Ivanenko et al., 2004). However when the movement involves the whole body as during a reaching from a standing posture the muscle coordination becomes trickier.

Recent kinematic studies performed on whole-body pointing movement, (Berret et al., 2009; Kaminski, 2007; Thomas et al., 2005) revealed a decrease of dimensionality in the kinematic and kinetic spaces. Joint co-variation characterized natural whole-body pointing movements while a synergistic and modular organization of upper versus lower-limb joint displacement emerged when pointing constraints were imposed in the task (Berret et al., 2009). A kinematic coordination can however be the result of very different activation patterns of lower and upper-limb muscles. During a whole body pointing the reciprocal effects of the reaching sub-task with the equilibrium sub-task are complex. Thus, functionally different muscles can come into play at different phases of movement resulting in several combinations of muscle bursts.

Beside a description in term of co-variations between muscles of virtually all segments of the body, a synergy can also be defined as a temporal sequence of bursts of identified muscles. The well-known triphasic pattern recorded during a single-joint movement illustrates this distinction: a first burst of the agonist is followed by a burst of the antagonist and finally by a co-activation of both (see Berardelli et al., 1996). In that case, if calculated the co-variation between the agonist and antagonist muscle activities would be very low. In more complex tasks, Crenna and Frigo (1991) recorded a specific deactivation/activation muscle pattern before the reaching onset which is dedicated to offsetting the mechanical perturbation induced by the focal limb movement. Subsequent sequences of independent activity of trunk plus legs and arm

0306-4522/10 $ - see front matter
doi:10.1016/j.neuroscience.2010.07.006

muscles usually follow, allowing target achievement and final centre of mass stabilization.

These two meanings of muscle synergy (high level dimensionality reduction and single joint agonist/antagonist muscle grouping) might be compatible in the frame of a hierarchical schema. Physiological evidences for a modular spinal motor system in animal (Saltiel et al., 2001; Giszter et al., 1993; see Bizzi et al., 2008 for a review) and recently in human (Cheung et al., 2009) suggest that goal oriented tasks rely on muscle pattern specified by networks in the spinal cord, as for locomotion (Grillner, 1985). In this context, the previous grouping of kinematic variables (Berret et al., 2009) could reflect a basic organization in the muscle space, where descending cortical command would be converted by a pattern generator in subcortical and spinal structures to activate synergistically lower and upper limb muscles.

In light of this possibility, we recorded the EMG activities from up to twenty-four subjects' body muscles during a pointing task beyond arm's length to answer several questions: Is dimensionality reduction associated with whole-body pointing movements described in the kinematic and kinetic spaces also present in the muscle space? If a dimensionality reduction in muscle space is verified, does it correspond to a synergic activity of identified agonist/antagonist muscles? In addition to natural whole-body pointing movements, further conditions were considered in this study in which specific spatial or equilibrium constraints were applied to either upper or lower-limbs (as in Berret et al., 2009). In this way it was tested if the muscle organization associated with unconstrained natural movements was robust and invariant or dependent on the task. Indeed, the introduction of such constraints could result in a completely new muscle organization driving simultaneously all-body muscle or, alternatively, in the modification of the patterns of activation of only local groups of muscles (for instance those acting at each body joint).

The results revealed a robust reduction of the whole electromyographic activity to a tri-dimensional and triphasic muscle patterns, distributed as a functional unit at each joint and independent of constrains' imposition. Preliminary results of these findings were previously published in abstract form (Chiovetto et al., 2008).

EXPERIMENTAL PROCEDURES

Participants

Twelve healthy male subjects (ages 29±4 years, mass 74±9 kg, height 1.77±0.07 m), participated voluntarily in the experiment. All subjects were in good health condition and had no previous history of neuromuscular disease. The experiment conformed to the declaration of Helsinki and informed consent was obtained from all the participants according to the protocol of the local ethical committee.

Protocol

Participants were required to point with both their index fingers the extremities of a wooden dowel (45 cm long, 3 cm of diameter) located in front of them. It was positioned horizontally with respect to the ground, parallel to the subjects' coronal plane and with its centre intersecting the subjects' sagittal plane. For each participant, the extremities of the dowel had a vertical distance from the ground equal to 15% of their body height. Two horizontal target distances (measured starting from the distal end of the participants' great toe) were tested: the first one (D1) corresponded to 5% of participants' height, the second one (D2) to 30%. Increase of target distance could indeed result in a change of the general muscle organization, being for such condition the equilibrium demand much higher for the condition with target at D1. Participants started from an upright standing position with their hands initially located at the external side of the thighs and thus induced hand-pointing movements in a semipronated position. The whole movement, that was assumed to be symmetrical (Kaminski, 2007), was performed in the sagittal plane with each side of the body moving together. After verbal instruction that data recording had started, participants had to perform a natural pointing task (not too slow or too fast to induce loss of balance) and to stop at the end of the movement, keeping the fingers close to the bar until verbal indication from the experimenter that the acquisition had been stopped. Target accuracy was not the primary constraint during the experiments and no instruction was given to the participants regarding the strategy to follow to accomplish the pointing; indeed, due to the large number of degrees of freedom involved in the task, the target could be reached in many different ways (e.g. with or without flexion of the knees, with or without trunk bending, by moving first the arms and then the trunk plus lower limbs, etc.). Each subject performed one block of six valid trial repetitions for each target distance. By not imposing any constraints, our goal was to study whether, when performing a whole-body pointing movement naturally, a predominant motor strategy among all the possible ones existed across the participants.

Additional conditions

Two additional conditions were performed, by the same group of subjects, to verify whether the introduction of a postural or pointing constraint could change the global muscle strategy associated with whole-body pointing movements, if one existed. In particular, during the experiment, subjects were asked to reach the target without flexing the knees or drawing a large and semicircular trajectory with the index fingers, whose diameter was equal to the distance between the initial position of the fingers and the target. With the imposition of such local constraints we wanted to determine a change of the dynamics associated with at least some body-joints and consequently to determine also a modification of the activation patterns of some groups of muscles. For both additional conditions the target was positioned at longest distance, which was 30% of participants' height. In the rest of the manuscript we will refer to these two as knee (K) and imposed trajectory (IT) conditions. Subjects performed one block of six trial repetitions for both K and IT after performing conditions D1 and D2.

Apparatus

During trial executions, kinematic, dynamic and EMG data were simultaneously monitored. Body kinematics was recorded by means of a Vicon (Oxford, UK) motion capture system while subjects stood in upright position on an AMTI (Watertown, MA, USA) force platform that measured torques and forces, as well as the motion of the centre of pressure under the feet. Eleven passive markers were attached on the right side of the participant's body on lower limb (fifth metatarsophalangeal joint of the foot, lateral malleolus, knee interstitial joint space, greater trochanter, iliac crest), arm (the acromion process, lateral epicondyle of the humerus, the styloid process and the tip of the index finger) and head (external canthus of the eye and auditory meatus). This marker configuration allowed schematizing the human body as a multi-joint system made of seven segments (as depicted in Fig. 1):

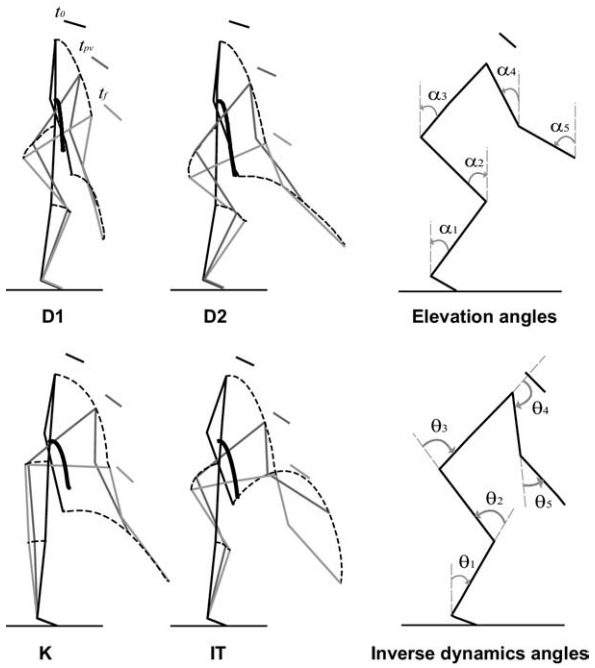

Fig. 1. Typical stick diagrams for the two main conditions (normal pointing with target at short and long distance, respectively D1 and D2) and the control conditions K (no knee flexion) and IT (imposed curved trajectory of the index fingers). Seven main segments modelling subject's body are shown at three different instants of time: finger movement onset t_o, instant of maximum peak of velocity t_{pv} and end of the movement t_f. The trajectories of knee, hip and shoulder markers (black dashed lines) and global CoM (black thick solid line) are traced. The two stick figures on the most right panels define the elevation angles and the angles θ_i used for the inverse dynamics analysis. Positive angles always indicated counter-clockwise rotations.

head, trunk (thorax plus abdomen-pelvis), thighs (as a single segment), shanks, feet, upper arms and forearms. Based on this model, the position of the global body centre of mass was computed by means of standard methods and by using statistical anthropometric data (Winter, 1990). The model and the method used to estimate the whole-body centre of mass (COM) trajectory were already validated in previous studies (Stapley et al., 1999). Marker positions were used to compute the kinematics of the index finger and torques at the joints, as well as the time series of the elevation angles of the different body links. Kinematic and force platform data were recorded at a sampling frequency of 100 Hz. Electromyographic activity was monitored by means of an Aurion (Milan, Italy) wireless electromyographic system. Impedance between the surface electrodes was always checked not to exceed 5 kΩ: in the case of higher values, skin was rubbed by means of an abrasive sponge in order to decrease it. EMG data were amplified (gain of 1000), band-pass filtered (10 Hz high-pass and 1 kHz low-pass) and digitized at 1000 Hz. Up to twenty-four different muscles from the right hemibody were simultaneously recorded: tibialis anterior (Tib), soleus (Sol), peroneus (Per), gastrocnemius (Gast), vastus lateralis (VL), biceps femoris (BF), vastus medialis (VM), semitendinosus (ST), rectus femoris (RF), semimembranosus (SM), adductor longus (AL), erector spinae (ES), rectus abdominis (RA), gluteus maximus (GM), internal oblique (OI), latissimus dorsi (LD), serratus anterior (Ser), anterior deltoid (DA), posterior deltoid (DP), pectoralis superior (Pect), rhomboid major (Rho), biceps brachii (Bic), triceps brachii (Tri) and brachioradialis muscle (Bra). The functional role of each single muscle and the right placement of the electrodes were tested by making subjects perform both isometric and free movements (Kendall et al., 2005). When accomplishing whole-body pointing movements, the pointing subtask is mainly carried out by the shoulder muscles. Additionally, knee and trunk flexions contribute to the subtask as well, by moving the shoulders toward the target. Thus, from now on and for the sake of simplicity, upper-limb muscles will refer to those muscles acting on arms and shoulder joints (Bra, Tri, Bic, Rho, Pect, DP, DA, Ser, LD); lower-limb muscles will refer to the rest of the muscles of the body (Tib, Sol, Per, Gast, VL, BF, VM, ST, RF, SM, AL, GM, OI, RA, ES).

Data analysis

Data were analyzed off-line using customized software written in Matlab (Mathworks, Natick, MA, USA). Kinematic and force platform data were low-pass filtered (Butterworth filter, cut-off frequency of 20 Hz). Marker velocities and accelerations were obtained by numerical differentiation of their spatial positions. Torques exerted by muscles at ankle, knee, hip, shoulder and elbow joints were derived with an inverse dynamic analysis in the sagittal plane (details are given in Appendix). For the EMG analysis, muscle signals were full-wave rectified, normalized in amplitude with respect to their maximum value recorded across all trials and conditions and low-pass filtered once more with a zero-lag Butterworth filter and a cut-off frequency of 10 Hz. To test the effects of the filter cut-off frequencies on some parameters of the analysis, some rectified EMG datasets were also filtered at 30 and 100 Hz. The level of muscle activation recorded is always dependent on many variables, such as movement velocity and skin impedance between the electrodes: this operation of normalization allowed comparing and averaging muscle recordings across trials and subjects. The time instant t_0 with respect to which the muscle activation and deactivation onset delays were computed for every trial corresponded to the pointing movement onset, at which the bell-shaped velocity profile of the right index finger exceeded 5% of its peak value. For each rectified EMG signal the deactivation or activation onset delays (called respectively offsets and onsets) in a time interval about t_0 were determined, when they existed, by computing the difference between the instant of movement initiation and the time at which the rectified EMG amplitude exceeded its mean level (computed between −300 and −100 ms prior to t_0) plus two standard deviations (in the case of activation) or decreased below the mean level minus one standard deviation (for deactivation) and remained respectively above or below such thresholds for at least 30 ms. For activations, two standard deviations instead of one were chosen to avoid confusing actual muscle activations with slight changes of the tonic activity level (Stapley et al., 1999) or spikes due to noise and affecting the muscle baseline at rest. For deactivation onset, the minimum time duration of 30 ms during which a rectified EMG signal had to remain under the threshold assured that the one recorded was really a deactivation from a tonic activity. Indeed, if the muscle was not active and the one recorded was just the muscle baseline when it was relaxed, muscle activity could not likely drop below such a threshold for a so long time period. Finally, in order to compute the average muscle activity across trials or subjects, the filtered EMG signals comprised between 300 ms before t_0 and 100 ms after the end of the movement were normalized to a standard time window of 1000 samples, with the end of the movement defined as the instant t_f at which the index finger velocity profile dropped below 5% of its peak value (reached at instant t_{pv}).

Among the twenty-four muscles recorded during the experiment for every participant, some showed a change in signal amplitude (because of the imperfect adhesion of the electrodes to the skin) and were excluded from further analyses (see Table 1). However, such a removal did not have any considerable effect on the results. Indeed, analyses were performed by working on average (across either subjects or trials) parameters.

Table 1. List of muscles monitored for each single participant

Muscles	AM	AP	AS	BB	CM	EC	JS	LD	LL	LM	MB	MJ
Tib	x	x	x		x	x	x		x	x	x	x
Sol	x	x	x	x	x	x	x	x	x	x	x	x
Per	x	x	x	x	x	x	x	x	x	x	x	x
Gast	x	x	x	x	x	x	x	x	x	x	x	x
VL	x			x		x	x	x	x		x	x
BF		x	x	x		x	x	x	x	x	x	x
VM	x			x	x	x		x	x		x	x
ST	x	x	x	x	x	x	x	x	x	x	x	x
RF		x		x	x	x		x	x		x	x
SM		x	x			x	x	x	x	x	x	x
AL	x	x						x	x	x	x	x
ES				x			x		x	x	x	x
RA	x	x		x			x			x		
GM					x	x	x		x			x
OI	x	x	x	x	x	x	x	x	x		x	x
LD	x	x	x	x	x	x		x	x	x		x
Ser	x	x	x	x	x	x	x	x		x	x	x
DA	x	x	x	x	x	x	x	x	x	x	x	x
DP			x	x		x		x	x	x	x	x
Pect	x	x	x	x	x		x	x	x	x		x
Rho	x	x	x	x	x	x	x	x	x	x	x	
Bic	x	x	x	x	x	x	x	x	x	x	x	
Tri	x	x	x	x	x	x	x	x	x	x	x	x
Bra	x	x	x	x	x	x	x	x		x	x	x

Muscle crosstalk

Surface EMG electrodes were attached on each muscle by following standard recommendations and procedures, as indicated by Hermens et al., (2000). Nevertheless, contamination of the EMG muscle signals by the activations of other adjacent muscles could be possible and the amount of such contamination had to be assessed. Cross-correlation analysis between channels revealed that the average peaks of the cross-correlation function in an interval about lag zero never exceeded 0.3. Because of the difficulty of distinguishing between muscle crosstalk and synchronous recruitment of motor units in different muscles (d'Avella et al., 2008; Kilner et al., 2002) we did not excluded such muscles from further analyses. Thus, we verified that results obtained by working on different subsets of data in which muscle potentially affected by crosstalk were removed did not change significantly. Finally, we tested the absence of muscle cross-talk also by providing a small control experiment in one single subject. We provided electrical stimulation to the RF muscle of his right leg and recorded the activities of the VL and VM, which are muscles adjacent to the RF and could be the main locus of crosstalk effect. After stimulation, only RF presented clear muscle activation induced by the electric impulse, while for VL and VM no activity was recorded. This observation confirmed that the effect of muscle cross-talk on the global muscle activity could be considered minimal and negligible.

Principal component analysis (PCA) and non-negative matrix factorization (NNMF)

PCA was first applied to kinematic and kinetic data to test whether our experiments confirmed the results obtained in previous works (Berret et al., 2009; Thomas et al., 2005) focusing on studying the reduction of dimensionality in the space of the elevation angles and in that of the joint torques. Kinematic and kinetic measures associated with each single trial of each participant were time-interpolated to fit a standard 200-point time base, pooled together and PCA was then applied to their covariance matrixes. PCA was also used to remove the intrinsic noise of measure affecting filtered EMGs. To this aim, PCA was applied to filtered EMGs and the cumulative percentage of variance accounted for (VAF) was computed as a function of the number of principal components (PCs) considered. The dimensionality D of the dataset was determined as the number of components at which the graph of the cumulative VAF presented a considerable change of slope (an "elbow") and after which the slop of the graph became constant (Ferré, 1995). The exact point of change was quantitatively determined as the point at which two consecutive segments connecting adjacent points on the graph formed the smallest obtuse angle. Filtered EMGs were finally reconstructed and freed of noise by using just the first D extracted PCs. Since low-pass filtering has usually a smoothing effect on the signals, possible influences of different cut-off frequencies on the dimension D of the analyzed EMG dataset were tested. Therefore, PCA was applied to three separate datasets that derived from the same initial rectified EMGs that were low-pass filtered at three different frequencies (respectively 10, 30 and 100 Hz). Obtained results were then compared. To identify specific patterns of activation characterizing the different muscle datasets, de-noised filtered EMGs were applied a customized version of the NNMF algorithm proposed by Lee and Seung (1999), and based on the minimization of the cost function below

$$E^2 = \sum_{k=1}^{T} \|m(t_k) - \sum_{i=1}^{N} c_i(t_k) w_i\|^2$$

subject to the constraints $0 \leq w_{ij}$, $c_i(t) \leq 1$ and where T is the total number of time samples, $\boldsymbol{m}(t_k)$ is a vector of M real numbers whose elements are the activations at the instant t_k of the muscles taken into consideration, the $c_i(t_k)$ ($i=1,2,\ldots,N$) are the combination coefficients and the w_{ij} ($i=1,2,\ldots,N$, $j=1,2,\ldots,M$) are the elements of the basic time-invariant vectors of muscle activations (or muscle patterns) w_i. The number N of combination coefficients and muscle vectors is a parameter of the analysis and it can be set arbitrarily by the experimenter. Here, it was decided to set the number N of components based on the PCA results and consequently to fix it equal to the dimension D provided by PCA performed over the filtered EMG dataset under investigation. The invariance of N from the specific matrix factorization algorithm was previously demonstrated (Ivanenko et al., 2005; Tresch et al., 2006) so as to make our choice of N licit. Tresch and colleagues stated that, among the methods they compared to extract muscle synergies, "the best algorithms were independent component analysis (ICA) applied to the subspace defined by PCA." The rationale for the combined use of PCA and NNMF here was similarly to benefit of the easiness of interpretation of the NNMF results derived from the low-dimensional space provided by PCA. After setting the muscle patterns and combination coefficients to random initial positive values, the minimum was sought by iterating two consecutive steps. First, the combination coefficients were updated following a gradient-descent procedure and, second, the same was done for the elements of the muscle patterns w_i. The iteration of these steps was stopped as soon as the least-square error between the noise-free EMG signals obtained after PCA and the reconstructed ones was minimized. Furthermore, no dependence of the muscle vector patterns from the initial conditions was found since the same vectors were obtained over repeated optimizations starting any time from different random values of the $c_i(t_k)$ and w_{ij}.

This PCA plus NNMF algorithm was applied to different muscle datasets. It was applied, for D1 and D2 conditions, to the average filtered EMG activity of each single subject. PCA and NNMF were also applied, for each condition, to the dataset obtained by pulling together the average activities of all subjects. Finally the dependency of the results on the group of muscles considered was tested. PCA and NNMF were applied to the

Table 2. Mean values and standard deviations of finger, centre of mass kinematic parameters and angular displacements for all experimental conditions

	D1	D2	K	IT
Finger				
MD (s)	0.77±0.16	0.83±0.14	0.93±0.15	1.10±0.21
PV ($m \cdot s^{-1}$)	1.46±0.27	1.98±0.34	1.75±0.23	1.94±0.53
TPV (% of trial duration)	0.48±0.08	0.43±0.06	0.46±0.05	0.54±0.16
Centre of mass				
A-P (m)	0.05±0.02	0.09±0.02	0.12±0.02	0.12±0.03
Vert (m)	0.29±0.03	0.41±0.05	0.28±0.01	0.35±0.08
TPV (% of trial duration)	0.49±0.08	0.48±0.05	0.50±0.04	0.59±0.11
Angles				
Ankle (°)	17.03±8.91	24.57±10.29	13.80±3.75	16.81±10.85
Knee (°)	65.05±16.29	86.52±21.12	17.03±8.91	59.89±28.67
Hip (°)	103.65±8.68	122.63±8.21	101.46±6.52	116.18±27.74
Shoulder (°)	46.76±10.17	86.61±10.18	109.25±6.62	100.79±20.15
Elbow (°)	8.97±4.04	12.70±14.92	11.59±4.59	32.77±23.71

matrixes pooling together the average de-noised filtered EMG signals of each single subject of the muscles acting at each body joint. In particular, the specific groups of muscles considered were the following: Tib, Sol, Per and Gast for the ankle, BF, VL, VM, RF, ST and SM for the knee, RF, ST, SM, RA and ES for the hip joint, DA, DP, Pect and LD for the shoulder, Bic, Tri and Bra for the elbow.

Goodness of signals reconstruction and robustness of the NNMF outputs

The outputs of the NNMF algorithm were, after its execution, N elementary muscle vectors and N scalar time-varying combination coefficients. Since they resulted from a minimization algorithm, their use in the reconstruction process of the original data were consequently a source of some variability. It was thus important to quantify the goodness of reconstruction of the original data by means of the vectors and combination coefficients obtained from NNMF. The uncentered Pearson correlation coefficient R (cross-correlation function computed at lag zero) was used as an index to measure similarity between the recorded muscle activities and the corresponding one reconstructed by combining together the NNMF outputs. The correlation coefficients was also used to assess similarities between corresponding combination coefficients $c_i(t)$ extracted from different datasets. Note that, when computing such a coefficient, data are not subtracted by their mean values. As a consequence, R results suitable to evaluate similarities of both shape and magnitude of two signals (Torres-Oviedo et al., 2006) and a unitary value for R indicates a perfect matching between two signals. Such coefficient revealed thus appropriate to quantify if two muscle signals were characterized by similar level of baseline activity. Similarity between two muscle vectors $\boldsymbol{u}$ and $\boldsymbol{v}$ obtained from NNMF was tested by computing the scalar product S (whose values ranged between 0 and 1) of the two normalized vectors (see Cheung et al., 2005). A scalar product equal to 1 characterized two identical vectors.

Statistical analysis

A single factor analysis of variance (ANOVA) was applied to investigate statistical effects of the movement conditions on the kinematic parameters of motion. Student's t-test was used to study the influence of distance on activation and deactivation onset delays. Statistical differences among the percentages of VAF explained by a same number of PCs extracted from different data sets were also tested. The level of significance at which the null hypotheses were rejected was set at 5%. A chi-square goodness-of-fit test was used to test the normality of the delay distributions. A multiple comparison method (with Tukey–Kramer correction) was applied to test which pairs of means, among those relative to multiple normally distributed populations, were significantly different.

RESULTS

General characteristics of movements and inter-subjects variability

The mean values of some kinematic measures referring to the finger and body centre of mass motion were calculated and are reported in Table 2. Such values are in line with those already computed in previous works (Stapley et al., 1999; Pozzo et al., 2002; Berret et al., 2009), in which it was described in details how, for D1 and D2 conditions, subjects performed whole-body pointing movements in a very stereotyped way. More specifically, authors showed that the subjects' centre of mass and finger path toward the target were always characterized by an initial forward displacement along the horizontal direction followed by a downward displacement along the vertical direction. These findings are illustrated by the stick diagrams relative to one trial execution for each condition (see Fig. 1) and by the averaged time series of the elevation angles (Fig. 2A), which resulted similar to those presented by Berret and colleagues (2009) for all the four experimental conditions. For each subject, angular displacements were always found to be consistent across trials (standard deviation values always$<$4 degrees). Nevertheless, ANOVA analysis revealed interestingly that, within each condition, the mean values of the peak-to-peak angular displacements were always significantly different from subject to subject ($P<0.01$ for each angle), indicating that different joint strategies were used (in particular, with more or less knee flexion and trunk bending). Despite this variability, PCA performed on the angular displacements recorded during each single trial confirmed that a high level of co-variation existed among angles for both D1 and D2 and for all subjects, while a noticeable decrease of co-variation was found for condition IT (Fig. 2B), again for all subjects.

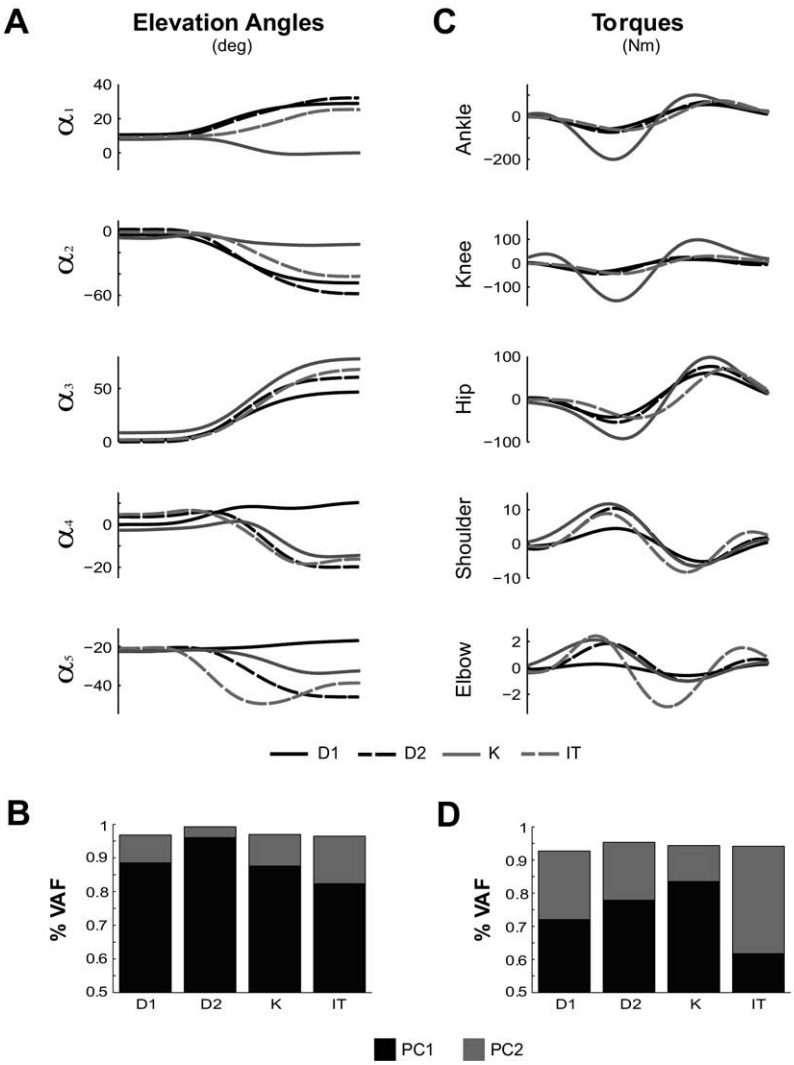

Fig. 2. (A) Time series changes of the average elevation angles for each condition. The reported average measures fit a standard 200-samples time windows. (B) For each condition, percentage of VAF by the first two PCs extracted from the elevation angles associated with the experimental trials. (C) Time series of the average torques at the joints. Positive torques determine counter-clockwise rotations. (D) Percentage of VAF by the first two PCs extracted from the torques at all joints.

Another parameter dependent on subjects was the time taken to reach the peak velocity of finger and centre of mass in Table 2 (both expressed as percentage of trial duration): ANOVA analyses within each condition revealed *P*-values always much smaller than 0.01. Therefore, even if whole-body pointing movements were shown to be characterized by global standard kinematic features (centre of mass and finger trajectories in the sagittal plane and joint coupling), they also presented some inter-subject variability in both temporal (time to peak velocity) and spatial (peak-to-peak joint displacements) domains. Time series of the average dynamic torques for each joints and conditions are reported in Fig. 2C. They presented biphasic shapes and, in accordance with Thomas and colleagues (2005), two components were required to explained most of their variance (Fig. 2D). Note that the condition characterized by the highest level of torque co-variation (highest value of VAF captured by the first PC) was condition K: indeed avoiding flexing the knees likely contributed to simplify body dynamics and to apparently decrease the degrees of freedom of the system, given that shank plus thigh could be thought as a single segment. In contrast, the condition in which the second PC contributed the most to the total variance (with the consequence of reducing torque co-variation) was condition IT, in which a strong reaching constraint was introduced.

General characteristics of the muscle activity

Fig. 3A illustrates the raw muscle activity for participant MJ (one among the participants of the main experiment who had the largest number of good muscle signals recorded simultaneously) during one single trial performed at D1. Anticipatory muscle activities preceding finger movement onset were clear. In particular, prior to t_0, the deactivation of a group of postural muscles (Sol, BF, ST, ES and SM)

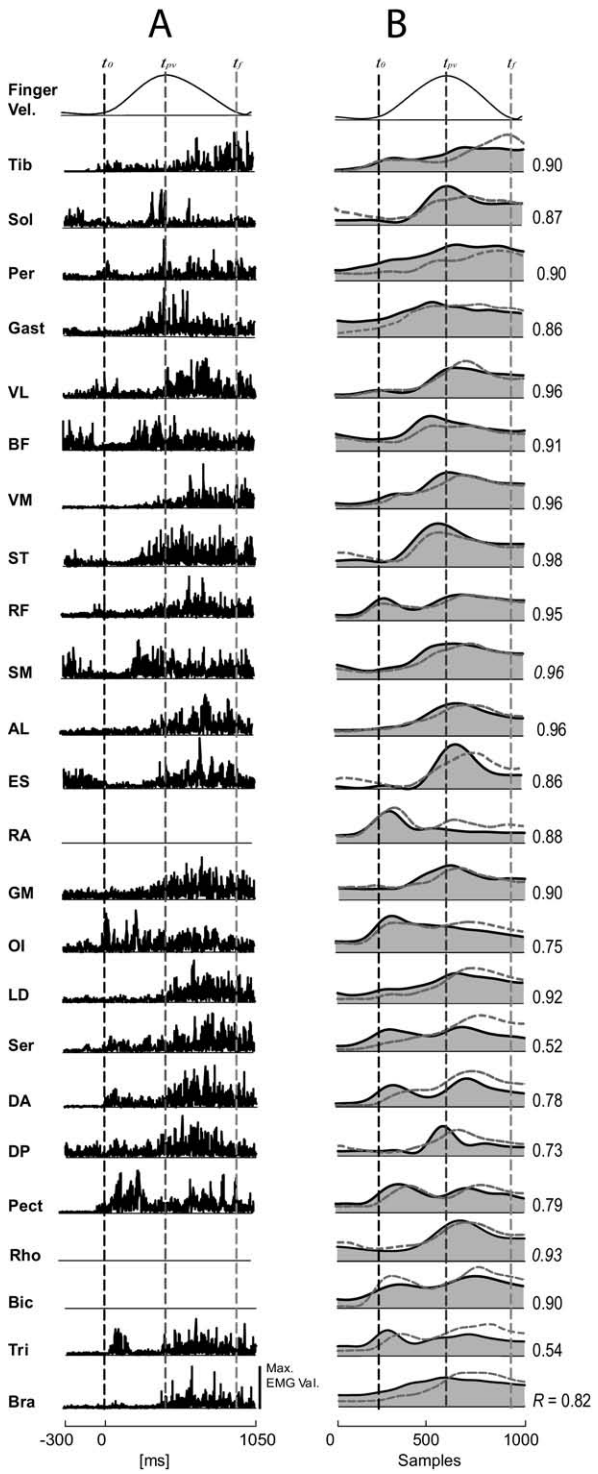

Fig. 3. (A) Raw muscle activity of a typical subject recorded during one single trial with target at short distance. Muscles were ordered according to their spatial location on the body, starting from the muscle acting on the ankles and continuing with those acting on the knees, hip, shoulders and elbows. Plotted signals were just rectified and normalized with respect to their maximum values recorded over all trials. The three vertical dashed lines mark finger movement onset (t_o), the instant of its maximum peak of velocity (t_{pv}) and the final instant of its movement as defined on the finger velocity profile plotted on the upper right part of the figure. The time interval between 300 ms before movement onset and 100 ms after the end of the pointing was considered. RA, Rho and Bic are missing because, for this subject, such muscles were not considered in the analysis. In this figure and in all the next ones in which muscle activities are displayed, the upper limit of each vertical axis was set to the maximum EMG value of that muscle during the time interval displayed. (B) Ensemble-averaged activity patterns of all the twenty-four checked muscles recorded from 12 subjects (For each muscle and subject, filtered EMGs were averaged across trials referring to the same experimental condition). In black lines and shaded area are the patterns relative to the pointing with target at D1 and, superimposed in gray dashed lines are the ones relative to pointing with target at D2. Averaging filtered EMG signals across several trials implies the achievement of smoother waveforms that may determine a loss of information that, at the contrary, is clear when checking rawer data. In this figure for example, initial deactivations of ES and DP are not as clear as they are in Fig. 2. The same is valid for Rho, whose first notable event coincides with its activation after t_o rather than its deactivation prior to movement onset, as it was found from the raw data. *R*-values reported on the right sides of the activities in panel B indicate, for each muscle, the correlation coefficient between the activity with target at D1 and D2.

was accompanied by the activation of a second group of both lower-limb (Tib, Per, RF, OI) and upper-limb (Ser, DA and Pect) muscles. Note however that DP also deactivated before t_0 as a result of the initial shoulder extension to keep the hands on the external side of the thighs, imposed to each participant. Then, between t_0 and t_{pv}, a further set of muscles activated that either previously deactivated (Sol, BF, ST, SM) or started becoming active (Gast, VL, VM, Add L, GM, LD, DP, and Bra). The second half of the movement, starting after t_{pv}, was characterized by a significant tonic activity and co-contraction of all the muscles that likely contributed to stiffen the joints and stabilize the centre of mass. The qualitative observations described above for one single subject remained globally valid also when the average filtered EMG activity across all subjects was considered, as shown in Fig. 3B. Furthermore, the high mean values of the correlation coefficients reported on the right part of each average muscle activity illustrated in Fig. 3B demonstrate that the average muscle pattern associate to movements accomplished with the target at D2 was substantially the same than the one when the target was positioned at D1. Interestingly, the muscles more affected by the distant target were mainly located on the upper body part (OI, Ser, DA, DP, Pect and Tri) and corresponded to a delayed action compared to the pattern recorded at D1.

PCA and NNMF

Global analysis. PCA was conducted over the average filtered EMGs (mean across trials) of all single participants pooled together, either for condition D1 and D2. Results revealed that, in the graph of the cumulative VAF, a clear and unequivocal elbow happened (following the criterion presented in the methods section) in correspondence of a number of components equal to three (Fig. 4A). The percentage of VAF was, for any number of components considered, always higher for PCs extracted from the D2 dataset. To test whether the cut-off frequency characterizing the low-pass filter had an influence on the eval-

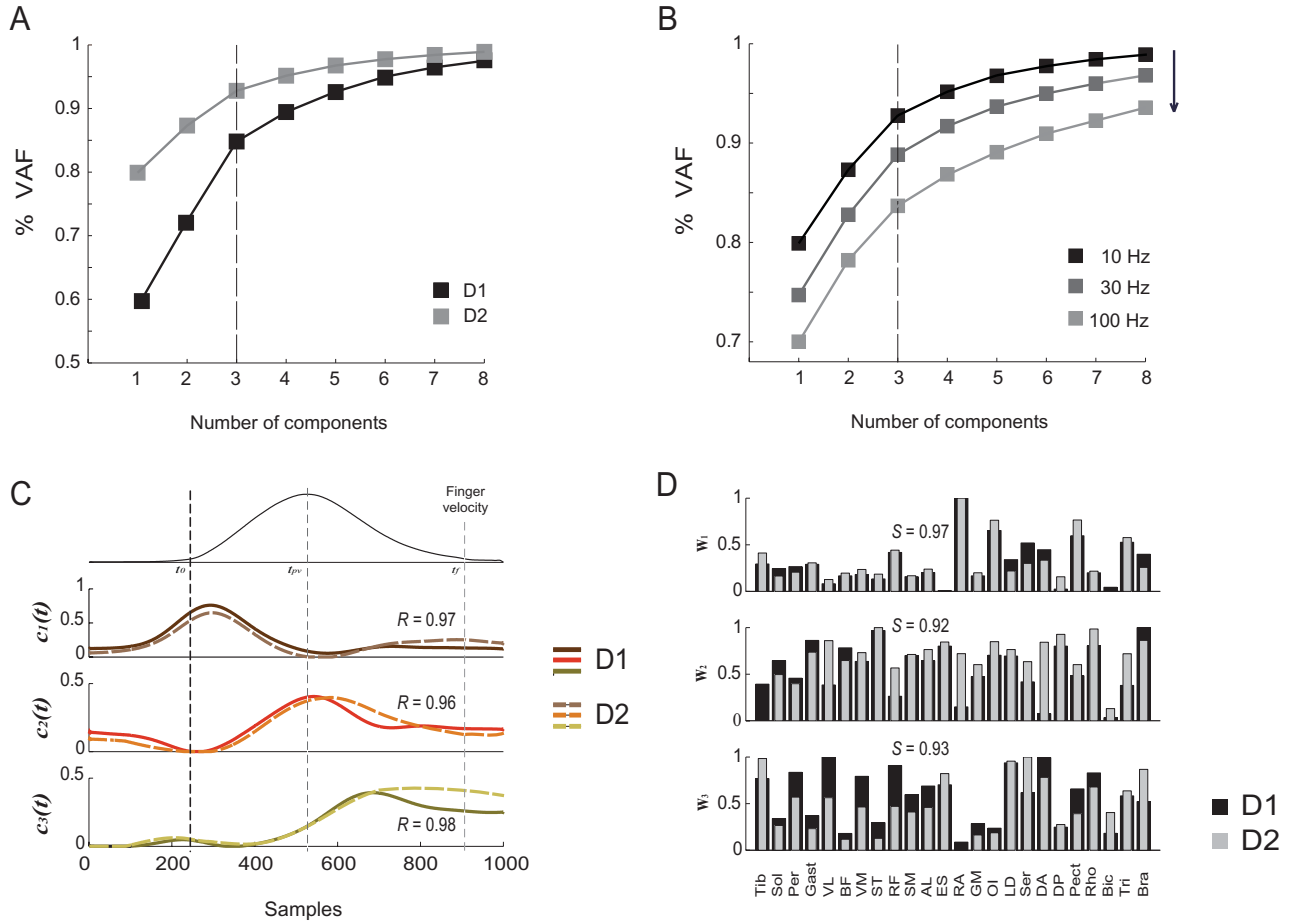

Fig. 4. (A) Variance account for (VAF) as a function of the number of principle components for condition D1 (black squared) and D2 (gray triangles). (B) Cumulative percentages of VAF from PCA performed on the average activities of all single subjects relatively to condition D2 and low-pass filtered at three different cut-off frequency values. In both (A) and (B) the vertical dashed lines indicate the number of component at which the biggest change of slope (elbow) occur. (C) Time courses of the average index finger velocity profile and the combination coefficients $c_1(t)$, $c_2(t)$ and $c_3(t)$ for both D1 and D2 conditions are shown (solid lines for D1, dashed light lines for D2). (D) Muscle vectors associated with the combination coefficients of Fig. 5B. Note that any muscle can be active in more than one vector with different activation levels. The *S* values reported indicate the level of similarity between the corresponding muscle vectors of condition D1 and D2. Their values are always higher than 0.9, indicating no substantial difference in the muscle activity when reaching the target at different distances.

uation of the dimension of the filtered EMG dataset analyzed (or, in other words, on the number of components at which the elbow took place), PCA was performed on the EMG dataset relative to condition D2 filtered also at both 30 and 100 Hz. From direct inspection of the graphs in Fig. 4B depicting the cumulative percentage of VAF for each cut-off frequency, no significant effect of the cut-off frequency on the number of components was found. The most significant change of slope indeed, always happened for a number of components equal to three. Conversely, as the cut-off frequency increased, the percentage of VAF decreased of a roughly constant amount, whatever was the number of components considered.

Fig. 4C shows the time course, normalized at 1000 samples, of the combination coefficients $c_i(t)$, i=1,2,3 (ordered according to the timing of their peaks) obtained by applying NNMF to the matrix pooling together the denoised average muscle activities of all single subjects: because of the previous considerations, N was set equal to three. Each one of them had a dominant role in one of the three time phases: $c_1(t)$ was the one mainly responsible for the initiation phase, $c_2(t)$ to muscle deactivations phases, and $c_3(t)$ to the final co-contraction of all muscles. Such contributions were not unique as conversely it might have been expected. In fact $c_1(t)$ contributed partly also to the co-contraction phase, as well as $c_2(t)$ and $c_3(t)$, that activated between t_0 and t_{pv}, played a role also in the braking one. This sharing of multiple contributions from different components by each time phase determined consequently the level of the muscle activations in each one of the three vectors w_i (Fig. 4D). Goodness of the identified outputs was proven by the computation of the correlation coefficients between each averaged muscle activation waveform and its corresponding one reconstructed by means of the three muscle vectors and combination coefficients identified. The average of the correlation coefficients associated with each muscle resulted R=0.94±0.05 for D1, R=0.91±0.07 for D2. Results resembling those reported

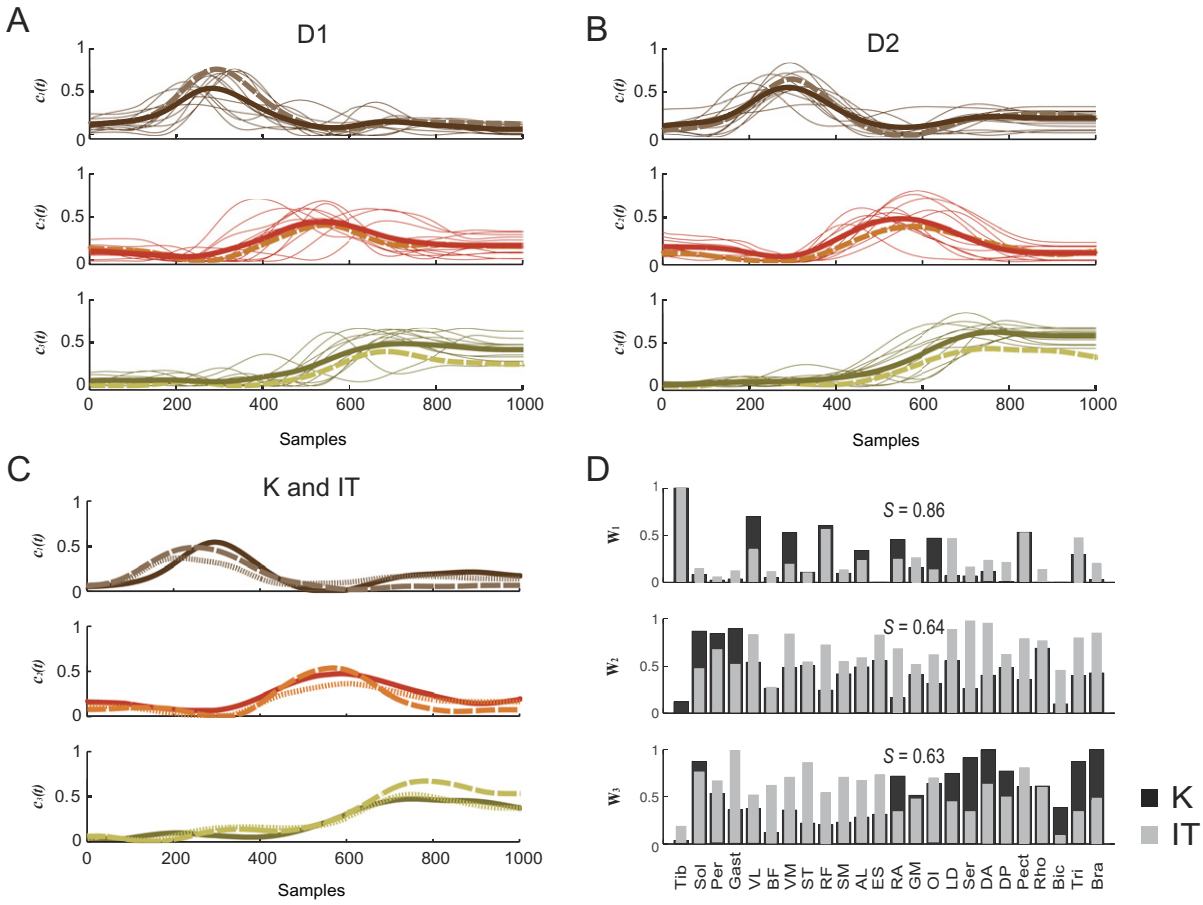

Fig. 5. (A) and (B) Combination coefficients extracted from each one of the 12 single subjects average muscle activities (thin lines) and their average values superimposed (solid lines) for condition D1 and D2. The light dashed lines represent the mean coefficients of Fig. 5B. (C) and (D) Combination coefficients and muscle vectors extracted from the average muscle activities (across all subjects and trials) of the control conditions K (dashed lines) and IT (dotted lines) superimposed to those of the condition D2 (solid lines). The *S* values of the vector products between corresponding muscle vectors relative to conditions K and IT are reported. Their values (much smaller than 1) underline substantial differences in the muscle activities of the two conditions, especially for the vectors associated with the second and third combination coefficients. Interesting is the behaviour characterizing the levels of activation of upper and lower-body muscles in the third vector. In condition K all lower-body muscles indeed present lower activation than in condition IT while, in opposition, in condition IT all upper-body muscle are less active than in condition K. This symmetrical behaviour of the two groups of muscles reflects the effects of the introduction of special constraints in movement execution.

in Fig. 4C, D were also obtained when applying NNMF to EMG signals filtered at 30 or 100 Hz. Fig. 5A, B illustrate that, for both target distances, the shapes of the combination coefficients extracted from the average filtered EMG activities of each single subject (thin solid lines) were very similar and asymptotic to the ones of Fig. 4C (thick dashed lines in Fig. 5A, B). The average correlation coefficients between the coefficient c_i from each single subject and those of Fig. 4B were respectively $R=0.90\pm0.02$ for $c_1(t)$, $R=0.83\pm0.08$ for $c_2(t)$ and $R=0.84\pm0.05$ for $c_3(t)$ for condition D1 and $R=0.91\pm0.01$ for $c_1(t)$, $R=0.89\pm0.02$ for $c_2(t)$ and $R=0.92\pm0.02$ for $c_3(t)$ for condition D2. Therefore, although some inter-subject variability existed, as shown by the correlation coefficients and probably due to the kinematic variability found across the participants, two main results could be extracted: the muscle space was three-dimensional and the underlying overall muscle activity was a triphasic muscle pattern.

PCA and NNMF were also applied also to the K and IT control conditions to test whether they were characterized by triphasic-like features as the robustness of the three-dimensionality and the triphasic characteristic of the muscle strategy. The introduction of a reaching or a postural constraint indeed, might influence the temporal organization of the three components associated to natural whole-body pointing movements. PCA revealed that for both K and IT conditions, three components could be considered to account for the variation of the two datasets. Results of NNMF applied to the average filtered EMG activities of all subjects pooled together for the two control conditions separately are depicted in Fig. 5C. Clearly the non-negative components extracted resulted in both cases similar to the one associated to condition D2. Correlation coefficients between those of condition K (IT) and D2 were $R=0.90$ (0.85) for $c_1(t)$, $R=0.98$ (0.96) for $c_2(t)$ and $R=0.95$ (0.97) for $c_3(t)$. Therefore the triphasic muscle pattern was robust

across conditions and different kind of whole-body pointing movements could be achieved by operating a re-weighting process at muscle level of three basic temporal components: muscle vectors for the K and IT dataset are shown in Fig. 5D.

The general strategy of combined muscle deactivations and activations described above was quantified by investigating the rectified EMGs of each subject recorded during each trials execution in condition D1 and D2 and by computing respectively muscle onsets and offsets. Fig. 6A depicts the mean offset values, plotted as percentages of movement duration. Sol, BF, ST, SM, ES and Rho deactivated almost

Fig. 6. Occurrence of muscle deactivations (offsets) and activations (onsets) calculated in all subjects and trials for the two target distances. (A) Average muscle offsets. Times are expressed in percentage of the movement duration. A negative time specifies that a muscle deactivate before t_0. (B) Average muscle time onsets. Red and blue indicate two separate groups of muscles activating respectively before and after t_0. For both (A) and (B), bars in darkest colours refer to condition D1, the lightest ones to condition D2. Asterisks indicate, for a given muscle, significant statistical differences ($P<0.05$) between average muscle offset or onset values relative to condition D1 and D2.

simultaneously for both D1 and D2 conditions. More specifically, multiple comparison tests revealed that only the BF average offset value was significantly earlier compared to ST and Rho for D1 while, for D2, DP offset was significantly different from those of BF, ST, SM (significance level set at 5% for both distances). The mean offset values for D2 were earlier than for D1 for ST and SM muscles ($P<0.05$). Fig. 6B plots muscle onsets. Data could be dissociated in two groups: the first one composed of muscles activating before finger movement onset and the second one having its elements activated after t_0. The overall strategy remained the same across conditions, except for Tib, Per, VM and VL that presented earlier onsets. VL activated even before movement initiation, becoming actively involved in the anticipatory activity. The reason of this change of strategy might be due to enhance the action of ankle flexors and knee extensors to produce greater backward displacement of the centre of pressure and, consequently, greater centre of mass forward acceleration (Stapley et al., 1999) because of the longest distance of the target. Also Pect and LD anticipated their onsets when the target was positioned at D2, but still remaining positive and consequent to t_0.

To sum up, the results showed that a stereotyped muscle activity was adopted by all subjects. Specifically, muscles were split in two separate groups acting synergistically: one made of a set of muscles (which, from now on, will we refer to as agonists) whose actions resulted in the generation of joint torques that accelerated the centre of mass forwards. These muscles were those with onset before finger movement initiation (negative values in Fig. 6A) and that produced ankle, knee hip and shoulder flexion. Note that such a definition of agonist muscles is a convention valid only in this study. Indeed, because of the complexity of the body kinematics, it is hard to know when a muscle is actually contracting to exert an “agonist” action: if one considered the biarticular muscles for instance, it is almost impossible to say if it is agonist or antagonist according to the usual definition. The other synergistic group (which, in contrast, we will refer to as antagonists) collected anti-gravitational muscles that either deactivated or activated respectively before and after the onset of the pointing motion. Temporally three phases were distinguished. The first one coincided with the successive deactivation of postural anti-gravitational muscles and activation of the agonists, which accelerated the body forwards and downwards (under the action of gravity). The second one occurred between finger movement onset and the instant of its maximum peak of velocity, in which the anti-gravitational muscles were recruited to slow down the movement of the centre of mass. The third one prolonged the previous sequence and corresponded to agonists and antagonist co-contraction to stabilize the whole body. Note that both upper and lower-limb muscles were present in each one of the three phases.

Local analysis. All the times that PCA plus NNMF were applied yielding the results presented above, all the muscles recorded during an experimental session were considered. Consequently, the number and the shape of the resulting combination coefficients represented the

most general muscle synergistic structure to obtain a set of different whole-body pointing movements. However, it remained unclear whether this global composition summarizing a large subset of muscles of all body segments was also effective at individual joints and for specific groups of agonist and antagonist muscles. This question makes sense with respect to the basic definition of a synergy as a group of muscles acting together at one joint (see Macpherson, 1991). For instance, the muscles acting at the ankle joint could exhibit (or not) the same three basic activation pattern. In addition, a different muscle pattern might be expected at certain joints of the lower or upper-limbs when performing whole-body pointing movements under postural (K) or focal (IT) constraints. To address this question a local analysis was performed. PCA plus NNMF were applied to five different groups of muscles acting respectively at the ankle, knee, hip, shoulder and elbow (see methods for the muscles belonging to each group). Analysis was repeated separately for condition D2, K and IT. PCA revealed again that filtered EMG datasets considered were always tri-dimensional (see Table 3 for the single values of percentage of VAF by each PC for each group of muscles and condition). In Fig. 7A are depicted, for each joint, the three combination coefficients extracted by NNMF and associated with the three experimental conditions studied. The high similarity of each triplet extracted with the global one relative to condition D2 and depicted in Fig. 4C is proved by the value of the average correlation coefficients between the time series of corresponding combination coefficients ($R=0.93\pm0.05$). Correlation coefficient values between the coefficients $c_i(t)$ of Fig. 7A and relative to normal condition D2, and the corresponding ones of condition K and IT are reported in Table 3. Their high values demonstrated that, at each joint, the temporal pattern of muscle activation was robust across conditions. Therefore, since the coefficients $c_i(t)$ did not show any modification across condition, also at local level different motor behaviour had to be obtained through a re-weighting process of the muscle vectors associated with the combination coefficients. To test this hypothesis the coefficient of similarity S was computed between the identified muscle vectors extracted from the dataset relative to condition D2 and the corresponding ones associated with K and IT conditions. Results are reported in histogram form in Fig. 7B. Low S values specify low similarity between corresponding muscle vectors of different conditions: high values, at the contrary, indicate that from one condition to the other the weights of the muscle vectors changed. From the histograms it is clear that, when considering D2 versus K, low values characterized the vectors of the lower-body joints: in particular, the lowest changes were found for w_2 and w_3 at ankle level and for all vectors at the hip joint. Note instead that small changes were found for the vectors of both shoulder and elbow joints (always $S>0.8$). Concerning D2 versus IT, the S values were, for the shoulder and elbow joints, always lower than those relative to D2 versus K, with a particular low level of similarity for all the three vectors of the shoulder joint (always $S<0.45$). Although the constraint imposed to subjects when accomplishing IT condition regarded mainly the reaching subtask, it determined also noticeable changes at the joints of the lower body (see in particular w_2 at the ankle and all the vectors at the hip). All together, histograms of Fig. 7B confirmed a reweighing in the muscle combination to perform different whole-body pointing movements according to an invariant triphasic muscle pattern. In particular, the introduction of a postural constraint changing the kinematic configuration of the lower-body joints (K condition) determined, with respect to the basic condition D2, a noticeable modification of the weightings of the ankle, knee and hip muscle vectors: in contrast the weights of the vectors associated with the upper-limb joints remained unvaried. Similarly, the introduction of the reaching constraint determined changes of the weights of the vectors of both shoulder and elbow joints but, in accordance to the idea that voluntary movement automatically induces postural perturbation, changes interested also the vectors of the lower-body joints, in particular ankle and hip.

Table 3. Table reporting, for each joint (and their corresponding muscles in parenthesis), the percentage of the VAF for the first three components (for D2, K and IT conditions) and correlation coefficients between corresponding combination coefficients of condition D2 and K and IT (Rc_1, Rc_2 and Rc_3)

Joint	Condition	% PC1	% PC2	% PC3	Rc_1	Rc_2	Rc_3
Ankle (Tib, Sol, Per and Gast)	D2	67.12	17.2	7.13			
	K	77.03	11.59	6.20	0.90	0.96	0.97
	IT	60.27	22.23	9.52	0.87	0.98	0.99
Knee (VL, VM, RF, ST and SM)	D2	72.49	14.28	7.47			
	K	48.42	26.07	15.73	0.97	0.99	0.97
	IT	64.16	19.35	8.52	0.96	0.96	0.94
Hip (RF, ST, SM, RA and ES)	D2	74.43	12.63	5.95			
	K	72.67	12.59	7.12	0.99	0.99	0.99
	IT	74.08	11.67	8.19	0.99	0.96	0.98
Shoulder (DA, DP, Pect and LD)	D2	75.62	12.50	5.27			
	K	78.76	5.24	7.00	0.99	0.95	0.99
	IT	77.83	10.66	5.69	0.93	0.90	1.00
Elbow (Bic, Tri and Bra)	D2	70.30	16.98	5.12			
	K	76.26	9.49	6.54	0.93	0.93	0.99
	IT	70.90	13.98	7.52	0.99	0.98	0.96

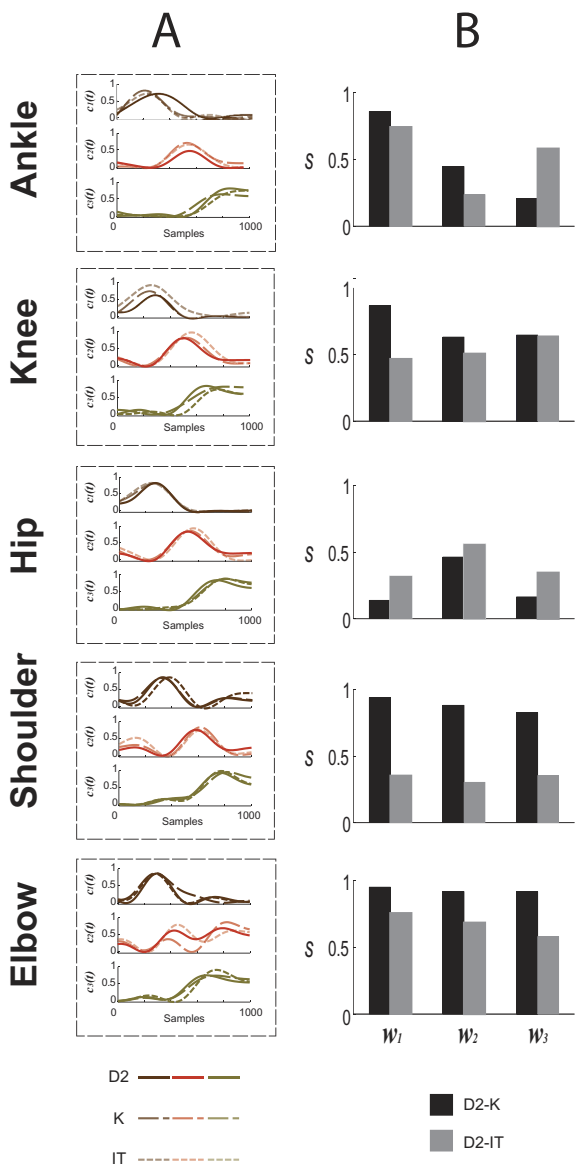

Fig. 7. (A) For each joint, the combination coefficients $c_i(t)$ ($i=1,2,3$) extracted by pooling together all single subjects' average activities of the muscles acting at that joint are illustrated. (B) Histograms reporting, for each joint, the indexes of similarity between corresponding muscle vectors w_i ($i=1,2,3$) of condition D2 and respectively K (black bars) and IT (light grey bars).

Finally the temporal evolutions of each combination coefficient across the body joints within each condition were compared. The goal of such an analysis was to investigate possible temporal changes of the same coefficients $c_i(t)$ at the different body joints: indeed, the imposition of movement constraints might introduce temporal shifts of the muscle activities, resulting in temporal changes of time series of the same coefficients $c_i(t)$. Polar diagrams reporting the cross-correlation values are shown in Fig. 8: a separation between lower-body (L) and upper-body (U) joints was made and included respectively ankle, knee and hip joints for L and shoulder and elbow joints for U. M_i ($i=1,2,\ldots,6$) indicated mixed pairs, that is pairs of joints in which one belonged to L and one to U. Cross-correlation coefficients were computed between all possible joint combinations. All the coefficients $c_i(t)$ were, for all conditions, highly correlated when considering pairs of L joints. However, the *R*-values dropped down considerably (see, for instance, M2, M4, M6 and U1 pairs relatively to coefficient $c_2(t)$ and condition K or M1, M5 and U1 for $c_1(t)$ and condition IT) when comparing corresponding combination coefficients of which at least one was relative to the elbow or shoulder muscle groups. Therefore, while the lower-body muscle groups were always characterized by a triphasic temporal pattern of activation independently of the condition considered, the ones relative to the upper-limb joints revealed being more flexible and dependent of the constrain imposed to the movement.

DISCUSSION

PC and NNMF analyses revealed that just three principal components could be used to explain more than 90% of the original variation associated with the twenty-four EMG signals recorded during a whole body pointing beyond arm's length. Our results extended those that have been obtained for different categories of human behaviours, like walking, arm reaching or equilibrium task (Ivanenko et al., 2004; d'Avella et al., 2006; Krishnamoorthy et al., 2003; Danna-Dos-Santos et al., 2008). This is in accordance with the hypothesis that the central nervous syetem does not control individual muscles but makes use of synergistically linked group of muscles (Lee, 1984; Macpherson, 1991; Kakei et al., 1994; Bizzi et al., 2008 for a review). More importantly, the combination of muscle activation extracted from the whole set of EMG data remained the same when separate groups of muscles acting at each body joint were considered.

Tri-dimensional and triphasic muscle organization

While the considerable number of degrees of freedom characterizing a whole-body pointing task leads to very different alternative joint strategies and muscle patterns, the activities of the twenty-four muscles recorded in the present study lay in a tri-dimensional hyper-plane and were temporally organized according to a triphasic pattern (three components, each one exhibiting one single peak of activation; these peaks were consecutive in time). This muscular organization was found to be robust across conditions (target distance and postural/focal constraints). Interestingly, a similar pattern is noticeable in several other studies that investigated the muscle activities but not their spatiotemporal organizations during movement comparable to whole-body pointing (Crenna et al., 1987; Cheron et al., 1997; Tyler and Karst, 2004; Leonard et al., 2009). By inspection of the typical muscle activity, it is possible to visually identify the three components extracted from our data. For instance in Leonard et al. (2009) simultaneous muscle deactivations and activations were clearly present before movement onset. This was followed by the activation of other muscles after motion initiation and finally tonic activity of some muscles when the movement approached to its end (Leonard et al., 2009, their Fig. 3B). This pattern

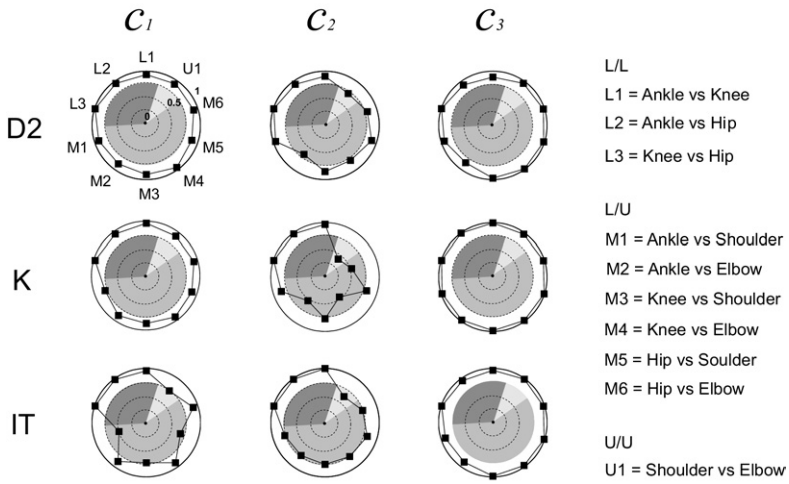

Fig. 8. Polar diagram reporting, for conditions D2, K and T, the correlation coefficient values between corresponding combination coefficient $c_i(t)$ ($i=1,2,3$) extracted at different joints. All the possible joint combinations were considered. The centre and the most external contour of each polar diagram corresponded respectively to the lowest ($R=0$) and highest ($R=1$) admissible values.

was independent of where the target was placed within a 180° array centered along the mid-line of the body.

Ivanenko et al. (2005) also found that three components were enough to reconstruct the activity of the twenty-nine muscles recorded during a similar stoop-in-place task. In particular, the first two components were found capturing about the 60% of VAF, while the higher order component resulted from trial to trial variability. The investigators explained the variability associated with the third component as a consequence of the impossibility to separate "two (or more) closely spaced activation events" that could not be resolved by their numerical method. More likely, the task specificity could explain such dependency (that we did not found) of the third component on trials. Stooping-in-place is a back and forth reaching with one single arm, contrasting from a discrete and downward whole-body pointing movement accomplished with both arms.

A striking result of our study is that the tri-dimensional temporal patterning of the twenty-four muscles was also present in the separate groups of muscles acting at each body joint. Seminal experiments have demonstrated that a fast single-joint arm movement is characterized by a similar triphasic muscle pattern of sequential bursts of activity of the agonist muscle, then of the antagonist and then of the agonist again (for a review see Berardelli et al., 1996). However, a similar standard pattern was a priori difficult to predict because of the biomechanical differences between a single-joint movement and the present multi-joint whole-body pointing task. This suggests that the present temporal architecture may represent a basic functional unit of the motor system. In favour of this hypothesis is the comparable distinctive pattern recorded in lower-limbs and trunk during arm raising (Friedli et al., 1984) or rapid voluntary body sway (Hayashi, 1998). For all these experiments the first agonist muscle bursts initiates the motion, the antagonist burst decelerates the movement toward the intended end position, and finally the second agonist burst stabilizes the limb after movement termination by dampening oscillations.

An important question is how and where the central nervous system can implement such a standard sequence of three temporal activation components available for multiple pairs of agonist and antagonist muscles in order to produce the present multi-joint reaching task. In a recent study performed with stroke patients Cheung et al. (2009) demonstrated the robustness of muscle synergies across arms and cortical lesions types. The authors concluded that cortical signals (from M1, premotor, supplementary areas or basal ganglia) would select, activate and combine in a flexible way specified networks in the spinal cord and/or in the brainstem, organizing each synergy. It might have been expected the muscle synergies identified by Cheung and colleagues to be characterized by a triphasic pattern of activation as well. However, in their work authors performed NNMF by pulling together not only EMGs collected during the accomplishment of simple free arm-reaching movements, but also those collected during the accomplishment of more complex constrained tasks such as reaching across multiple spatial constraints, shoulder circumduction or moving along a specific path. This determined an increase of the variability associated with the recorded datasets and a consequent increase of the number of synergies extracted. Likely, for some motor tasks, three among all the identified synergies could have presented profiles of activation in accordance with the acceleration, deceleration and stabilization phases described in this study and could have been enough to reconstruct at least the muscle activity of the recorded unconstraint reaching. However, the lack in Cheung's article of an explicit description of the time-varying coefficients relative to free one-shot movements does not allow verifying this last hypothesis. In consonance with this idea are the results of a previous study investigating the neural command that coordinates equilibrium and reaching subtasks in cat (Schepens and Drew, 2004). These authors reported three types of major signals in the discharge pattern of the reticular neurons in the pontomedullary reticular formation: (1) phasic

signals related to anticipatory postural adjustment, (2) phasic signals related to dynamic phase of the reaching movement, and (3) tonic signals related to postural stabilization. These three types of neurons are compatibles with the three temporal components identified here and of which the first two were phasic components and the third one was tonic. The authors proposed that the signals can originate from hierarchically higher regions of the central nervous system, converging on the pontomedullary reticular formation through the corticoreticular axons (Schepens and Drew, 2004; see also Dum and Strick, 2005).

On the basis of these considerations, we speculate that the triphasic muscle pattern found here would represent a fixed muscle synergy ensuring appropriate multiple agonist/antagonist muscles activation and operating at various level of the musculoskeletal system. Moreover, the neural organization encoding the triphasic muscle pattern would be specified by subcortical or spinal generators and activated by descending signals from motor cortical areas. This hypothesis is supported a fortiori by the robustness of the triphasic muscle pattern also present when constraints applied on the focal (IT condition) or the postural (K condition) subtasks induced new joint configurations. Interestingly, the reweighing of each component across muscles shown in IT and K conditions (see histograms of Fig. 7B) suggests flexible adjustments of the descending motor command that preserve the basic triphasic muscle pattern when the task requires a new kinematic strategy.

Hierarchical motor control

The present study points out a pyramidal organization of whole-body pointing control, which links together, in a single framework, the previous identified single kinematic dimension (Berret et al., 2009) to the present two and three dimensions relative to the kinetic and muscle spaces. Hence, the twenty-four muscles activity, reduced to a triphasic muscle pattern may be used to produce adapted joint torques and to manage kinematic goals (centre of mass and finger movements in extra-personal space). In the previous investigation (Berret et al., 2009) we hypothesized that angular displacements could be relevant task variables allowing a simultaneous control of the postural and focal subtasks (see also Lacquaniti et al., 1999). In light of this, the triphasic muscle pattern described here might represent the motor output of a neural controller that could manipulate the body geometry to generate a safe centre of mass displacement inside the base of support and a precise hand displacement toward the target. In this way, kinematic, kinetic and muscle variables could be specified in the same framework.

Todorov et al. (2005) described a hierarchical framework for "approximately optimal control of redundant systems" in which the main goal was to design a "high-level controller capable to exploit the natural plant dynamics while operating on a lower-dimensional system." Notably, the authors pointed out a relationship between the proposed hierarchical control theory and the feedback linearization property of a dynamic system (see subsection 4.1 in Todorov et al., 2005). When a system can be feedback linearized, it can be made linear and simplified just by operating a change of variable. Therefore, when accomplishing whole-body pointing tasks, the central nervous system might exploit this property (which is generally verified for a rigid-body kinematic chain), to consider the multi-joint system as a set of multiple single-joint rotations (neglecting interaction and gravitational forces), and to control each joint by using a standard motor synergy, for instance a triphasic muscle pattern. The minimum-energy wired-in synergy generator put forward by Neilson and Neilson (2005) in a form of a movement-to-muscle motor map also agrees with this assumption. More precisely, the central nervous system would select descending alpha drives integrating local functional properties of each basic synergistic unit (one agonist plus one antagonist). This hypothesis was especially verified for the lower limbs: these body parts exhibited very high angular co-variations (Berret et al., 2009) and a robust triphasic sequence of muscle activation (recorded here). Nevertheless, when required by the task, it seemed that a more flexible motor schema could be used to better control the end effector (as revealed by the muscle activity at the elbow joint).

CONCLUSION

The present investigation reveals that the central nervous system controls complex multi-joint movements using muscle synergies that have similarities with the control schema of single-joint flexion-extension. Both upper-limb and lower-limb muscles shared a stereotyped triphasic pattern, indicating a common control of the equilibrium and reaching subtasks, although a slightly more complicated muscular strategy was found in distal upper-body muscle groups. The key and novel insight regarding the mechanisms involved in the control of a multi-joint system is that, despite its prominent nonlinearity and high redundancy, we found the existence of a low-dimensional combination of muscle activity, compatible with the motion kinematics and kinetics. This possibly simplified the problem of constructing a motor command integrating the focal and the postural subtasks.

APPENDIX

Inverse dynamics analysis

We used Lagrangian analysis generally applied to robotic kinematic chains (Murray et al., 1994) to compute the muscle torques at the joints of the multi-link model of the human body that we have described above. This approach, which relies on the energy properties of a mechanical system, allowed us writing the system dynamic equations in a simple and closed form. We considered the vector $\boldsymbol{q} = (\theta 1, \ldots, \theta 5)$ of the joint angles as the vector of the generalized coordinates (see Fig. 1). After indicating as $T(\mathbf{q}, d\mathbf{q}/dt)$ the kinetic and $V(\mathbf{q})$ the potential energy of the system, we defined the Lagrangian L as

$$L(\boldsymbol{q}, d\boldsymbol{q}/dt) = T(\boldsymbol{q}, d\boldsymbol{q}/dt) - V(\boldsymbol{q})$$
$$= 1/2.d\boldsymbol{q}'/dt \,.\, M(\boldsymbol{q}) \,.\, d\boldsymbol{q}/dt - V(\boldsymbol{q})$$

where $M(\mathbf{q})$ was the inertia matrix of the multi-link model. Following the Lagrange's theorem, equations of motion were given by the Lagrange's equations

$$d(\delta L/\delta(dq_i/dt))/dt - \delta L/\delta q_i = \Gamma_i \; i = 1,.....,5$$

being Γ_i the vector whose elements were the external forces acting on the generalized coordinates q_i. By rearranging the results obtained from the previous equations, we could summarize the system dynamics as it follows:

$$\tau = M(\mathbf{q}) \, . \, d^2\mathbf{q}/dt^2 + C(\mathbf{q}, d\mathbf{q}/dt) \, . \, d\mathbf{q}/dt + N(\mathbf{q})$$

where τ was the vector of the muscle torques, C(**q**,d**q**/dt) the Coriolis/centripetal matrix and N(**q**) was the vector of the gravitational torques. To consider only the dynamic torques (Gottlieb et al., 1996) the value of the gravitational acceleration g was set to zero. The time course of the generalized coordinated was computed by means of trigonometric transformation of the Cartesian coordinates of the reflective markers on the participants. Angular variables and dynamic torques were positive when oriented counter-clockwise. The model was validated by comparing the identified torque at the ankles with the torque measured by the force plate under the feet. The two torques had indeed to equal one another, as it was assumed that the feet did not move during motion and could be considered as static rigid bodies.

Acknowledgments—The authors wish to thank Drs. Francesco Nori and Stefano Panzeri for precious comments on the earlier versions of the manuscript and Lilian Fautrelle and Marco Jacono for their help during data acquisition. Dr. Enrico Chiovetto's address at the time of publication: Section of Computational Sensomotorics, Hertie Institute for Clinical Brain Research and Center of Integrative Neurosciences, Tübingen, Germany.

REFERENCES

Berardelli A, Hallett M, Rothwell J, Agostino R, Manfredi M, Thompson PD, Marsden CD (1996) Single-joint rapid arm movements in normal subjects and in patients with motor disorders. Brain 119(Pt 2):661–674.

Berret B, Bonnetblanc F, Papaxanthis C, Pozzo T (2009) Modular control of pointing beyond arm's length. J Neurosci 29:191–205.

Bizzi E, Cheung VC, d'Avella A, Saltiel P, Tresch M (2008) Combining modules for movement. Brain Res Rev 57(1):125–133.

Cheron G, Bengoetxea A, Pozzo T, Bourgeois M, Draye JP (1997) Evidence of a preprogrammed deactivation of the hamstring muscles for triggering rapid changes of posture in humans. Electroencephalogr Clin Neurophysiol 105:58–71.

Cheung VCK, d'Avella A, Tresch MC, Bizzi E (2005) Central and sensory contributions to the activation and organization of muscle synergies during natural motor behaviors. J Neurosci 25(27): 6419–6434.

Cheung VC, Piron L, Agostini M, Silvoni S, Turolla A, Bizzi E (2009) Stability of muscle synergies for voluntary actions after cortical stroke in humans. Proc Natl Acad Sci U S A 106(46):19563–19568.

Chiovetto E, Nori F, Sandini G, Pozzo T (2008) Muscle synergies as a tool to study motor coordination between voluntary movements and posture. Soc Neurosci Abstr 960:15.

Crenna P, Frigo C (1991) A motor programme for the initiation of forward-oriented movements in humans. J Physiol 437:635–653.

Crenna P, Frigo C, Massion J, Pedotti A (1987) Forward and backward axial synergies in man. Exp Brain Res 65:538–548.

Danna-Dos-Santos A, Degani AM, Latash ML (2008) Flexible muscle modes and synergies in challenging whole-body tasks. Exp Brain Res 189(2):171–187.

d'Avella A, Fernandez L, Portone A, Lacquaniti F (2008) Modulation of phasic and tonic muscle synergies with reaching direction and speed. J Neurophysiol 100(3):1433–1454.

d'Avella A, Portone A, Fernandez L, Lacquaniti F (2006) Control of fast-reaching movements by muscle synergy combinations. J Neurosci 26:7791–7810.

Dum RP, Strick PL (2005) Frontal lobe inputs to the digit representations of the motor areas on the lateral surface of the hemisphere. J Neurosci 25:1375–1386.

Ferré L (1995) Selection of components in principal component analysis: a comparison of methods. Comput Stat Data Anal 19:669–682.

Friedli WG, Hallett M, Simon SR (1984) Postural adjustments associated with rapid voluntary arm movements 1. Electromyographic data. J Neurol Neurosurg Psychiatry 47:611–622.

Giszter SF, Mussa-Ivaldi FA, Bizzi E (1993) Convergent force fields organized in the frog's spinal cord. J Neurosci 13(2):467–491.

Gottlieb GL, Song Q, Hong DA, Almeida GL, Corcos D (1996) Coordinating movement at two joints: a principle of linear covariance. J Neurophysiol 75:1760–1764.

Grillner S (1985) Neurobiological bases of rhythmic motor acts in vertebrates. Science 228(4696):143–149.

Hayashi R (1998) Afferent feedback in the triphasic EMG pattern of leg muscles associated with rapid body sway. Exp Brain Res 119: 171–178.

Hermens HJ, Freriks B, Disselhorst-Klug C, Rau G (2000) Development of recommendations for SEMG sensors and sensor placement procedures. J Electromyogr Kinesiol 10:361–374.

Ivanenko YP, Cappellini G, Dominici N, Poppele RE, Lacquaniti F (2005) Coordination of locomotion with voluntary movements in humans. J Neurosci 25:7238–7253.

Ivanenko YP, Poppele RE, Lacquaniti F (2004) Five basic muscle activation patterns account for muscle activity during human locomotion. J Physiol 556 (Pt 1):267–282.

Kakei S, Muto N, Shinoda Y (1994) Innervation of multiple neck motor nuclei by single reticulospinal tract axons receiving tectal input in the upper cervical spinal cord. Neurosci Lett 172(1–2):85–88.

Kaminski TR (2007) The coupling between upper and lower extremity synergies during whole body reaching. Gait Posture 26:256–262.

Kendall FP, McCreary EK, Provance P, Rodgers MM, Romani WA (2005) Muscles: testing and function with posture and pain. Baltimore, MD: Williams & Wilkins.

Kilner JM, Baker SN, Lemon RN (2002) A novel algorithm to remove electrical cross-talk between surface EMG recordings and its application to the measurement of short-term synchronisation in humans. J Physiol 538:919–930.

Krishnamoorthy V, Latash ML, Scholz JP, Zatsiorsky VM (2003) Muscle synergies during shifts of the center of pressure by standing persons. Exp Brain Res 152:281–292.

Lacquaniti F, Grasso R, Zago M (1999) Motor patterns in walking. News Physiol Sci 14:168–174.

Lee DD, Seung HS (1999) Learning the parts of objects by non-negative matrix factorization. Nature 401:788–791.

Lee WA (1984) Neuromotor synergies as a basis for coordinated intentional action. J Mot Behav 16:135–170.

Leonard JA, Brown RH, Stapley PJ (2009) Reaching to multiple targets when standing: the spatial organization of feedforward postural adjustments. J Neurophysiol 101(4):2120–2133.

Macpherson JM (1991) How flexible are muscle synergies? In: Motor control: concepts and issues. New York, NY: Wiley.

Murray RM, Li Z, Sastry SS (1994) A mathematical introduction to robotic manipulation. Boca Raton, FL: CRC Press.

Neilson PD, Neilson MD (2005) Motor maps and synergies. Hum Mov Sci 24(5–6):774–797.

Pozzo T, Stapley PJ, Papaxanthis C (2002) Coordination between equilibrium and hand trajectories during whole body pointing movements. Exp Brain Res 144:343–350.

Saltiel P, Wyler-Duda K, D'Avella A, Tresch MC, Bizzi E (2001) Muscle synergies encoded within the spinal cord: evidence from focal intraspinal NMDA iontophoresis in the frog. J Neurophysiol 85(2):605–619.

Schepens B, Drew T (2004) Independent and convergent signals from the pontomedullary reticular formation contribute to the control of posture and movement during reaching in the cat. J Neurophysiol 92:2217–2238.

Stapley PJ, Pozzo T, Cheron G, Grishin A (1999) Does the coordination between posture and movement during human whole-body reaching ensure center of mass stabilization? Exp Brain Res 129:134–146.

Sugiuchi Y, Kakei S, Izawa Y, Shinoda Y (2004) Functional synergies among neck muscles revealed by branching patterns of single long descending motor-tract axons. Prog Brain Res 143:411–421.

Thomas JS, Corcos DM, Hasan Z (2005) Kinematic and kinetic constraints on arm, trunk, and leg segments in target-reaching movements. J Neurophysiol 93:352–364.

Todorov E, Li W, Pan X (2005) From task parameters to motor synergies: A hierarchical framework for approximately-optimal control of redundant manipulators. J Robot Syst 22(11):691–710.

Torres-Oviedo G, Macpherson JM, Ting LH (2006) Muscle synergy organization is robust across a variety of postural perturbations. J Neurophysiol 96:1530–1546.

Tresch MC, Cheung VCK, d'Avella A (2006) Matrix factorization algorithms for the identification of muscle synergies: evaluation on simulated and experimental data sets. J Neurophysiol 95:2199–2212.

Tyler AE, Karst GM (2004) Timing of muscle activity during reaching while standing: systematic changes with target distance. Gait Posture 20(2):126–133.

Welch TD, Ting LH (2008) A feedback model reproduces muscle activity during human postural responses to support-surface translations. J Neurophysiol 99:1032–1038.

Winter D (1990) Biomechanics and motor control of human movement. New York, NY: Wiley.

(Accepted 6 July 2010)
(Available online 13 July 2010)